Supporting Information

Unveiling Upsurge of Photogenerated ROS: Control of Intersystem Crossing through Tuning Aggregation Patterns

Junjun Wang, [a] Hao Li, [b] Yicai Zhu, [a] Mingdi Yang, [c] Jing Huang, [c] Xiaojiao Zhu, [a] Zhi-Peng Yu, *[a] Zhou Lu [b] and Hongping Zhou *[a]

[a]*School of Chemistry and Chemical Engineering, Institute of Physical Science and Information Technology, Anhui University and Key Laboratory of Functional Inorganic Materials Chemistry of Anhui Province, Anhui Province Key Laboratory of Chemistry for Inorganic/Organic Hybrid Functionalized Materials, Key Laboratory of Structure and Functional Regulation of Hybrid Materials (Anhui University) Ministry of Education, Hefei, 230601, P.R. China.*

[b]*Anhui Province Key Laboratory of Optoelectronic Material Science and Technology School of Physics and Electronic Information, Anhui Normal University, Wuhu 241002, China.*

[c]*School of Materials and Chemical Engineering, Anhui Jianzhu University, Hefei 230601, P. R. China.*

*Corresponding author.

E**mail:**

zhpzhp@263.net (Zhi-Peng Yu)

zpyu@ahu.edu.cn (Hongping Zhou)

Table of Contents

1. General Information on Materials and Methods

Materials. The chemical reagents: oxybis(ethane-2,1-diyl)bis(4-methyl-benzenesulfonate), (ethane-1,2-diylbis(oxy))bis(ethane-2,1-diyl)bis(4-methyl-benzene-sulfonate), 2-methoxyethanol, 2-(2-methyloxyethoxy) ethanol, 4-(diphenylamino)benzaldehyde, 4-methylbenzene-sulfonyl chloride, 4-methylpyridine, RB, ABDA, DMPO were purchased from Sigma-Aldrich, Aladdin or Adamas. The biological reagents: MTT, DCFH-DA, Annexin V-FITC /PI apoptosis detection kit, Mito-tracker Green, MDC and JC-10 got from reagent company (Thermo). The HepG2 (human hepatocellular carcinoma) cells were acquired from BeNa culture collection.

Characterization. ^{1}H-NMR and ^{13}C-NMR spectra of S-TPA-PI, S-2TPA-2PI, L-TPA-PI and L-2TPA-2PI were tested using Bruker AVANCE-400 MHz and 100 MHz NMR instruments with solvent of DMSO-d_6. Electrospray ionization mass spectrometric (ESI-MS) data were performed on Thermo Fisher Scientific LTQ-Orbitrap XL mass spectrometer. The UV-*vis* absorption and emission spectra for S-TPA-PI, S-2TPA-2PI, L-TPA-PI and L-2TPA-2PI were measured with UV-265 spectrophotometer and Hitachi F-4500 fluorescence spectrophotometer, respectively.

Preparation of solution. The four targeted compounds were dissolved in DMSO at a dilution of 10^{-3} M, and then diluted with distilled water or DMSO to 10^{-5} M for following testing.

$O_2^{-\bullet}$ detection. DMPO (20 mM) were severally added to the aqueous solution (10 μM) of S-TPA-PI and S-2TPA-2PI. The EPR signal was monitored by Bruker Nano x-band spectrometer without and with the LED lamp irradiation at room temperature.

$^{1}O_2$ detection. Firstly, ABDA (13 μL) were added to the aqueous solution (10 μM) of S-TPA-PI, L-TPA-PI, S-2TPA-2PI and L-2TPA-2PI, respectively. And then, under the LED lamp for various time, the UV-*vis* absorption spectra were measured immediately. The generation of $^{1}O_2$ in DMSO were measured at same methods.

Femtosecond transient absorption (*fs*-TA) spectroscopy. The *fs*-TA spectroscopy was acquired with a typical transmission pump-probe (UV-*vis* pump-broadband supercontinuum probe) instrument. All samples were excited at 420 nm and then probe with a WLC pulse ranging from 350 to 700 nm.

Cytotoxicity assessment (MTT assay). The cell viability of S-TPA-PI and S-2TPA-2PI in dark or light condition were tested with using HepG2 cells. Firstly, the experimental groups were packed up

with tinfoil or exposed upon the LDE light for 10 min (50 mW/cm^2). Then, 20 μL of MTT (5 mg/mL in PBS) and 200 μL of DMSO were added. In the end, the absorbance of 490 nm in each well were recorded on a Bio-Rad microplate reader.

Subcellular colocalization assay. HepG2 cells were plated onto confocal dishes (d = 35 mm) for 24 h at 37 ˚C. Next, the cells were treated with 10 μM S-TPA-PI, L-TPA-PI, S-2TPA-2PI and L-2TPA-2PI, staining with MitoTracker Green (10 μM), MDC or JC-10, respectively. And then, the as-prepared samples were visualized with laser confocal microscopy (Zeiss LSM980 and OLYMPUS FV3000 confocal laser scanning microscope). S-TPA-PI, L-TPA-PI, S-2TPA-2PI and L-2TPA-2PI (λ_{ex} = 488 nm, λ_{em} = 580 - 630 nm), MitoTracker Green (λ_{ex} = 488 nm, λ_{em} = 500 - 540 nm), MDC (λ_{ex} = 405 nm, λ_{em} = 490- 520 nm) JC-10 (green channel: λ_{ex} = 488 nm, λ_{em} = 520- 540 nm, red channel: λ_{ex} = 546 nm, λ_{em} = 560- 590 nm).

Cellular ROS production analysis. The HepG2 cells were incubated with 10 μM of S-TPA-PI and S-2TPA-2PI for 30 min, respectively. Following, 10 μM DCFH-DA were added. After that, the cells were washed with PBS three times and irradiated for 30 min. The green fluorescence was immediately observed using CLSM. (λ_{ex} = 504 nm; λ_{em} = 510-520 nm).

Photo-induced cell death mechanisms analysis. S-TPA-PI and S-2TPA-2PI (10 μM) were co-cultured with 400 μL dye diluent, 10 μL Annexin V-FITC and 5 μL PI in HepG2 cells under dark atmosphere for 15 min, respectively. Then the cell image was observed using CLSM. (Annexin V-FITC: λ_{ex} = 488 nm; λ_{em} =530 nm, PI: λ_{ex} = 543 nm; λ_{em} = 650-700 nm)

DFT calculations. The ORCA 4.2.0 software packages [S1] were used for all DFT computations assuming an S = 0 spin state. The geometry of the model complexes was optimized in the gas phase, employing the M06-2X functional [S2, S3] and RI/J Approximation [S4] without imposing any symmetry constraints. Geometry optimizations for the complexes were converged with the def2-TZVP/J auxiliary basis set [S1] for all atoms. Tight optimization and tight self-consistent field convergence were employed along with a dense integration grid (ORCA Grid 5) for all geometry optimization calculations. TD-DFT was carried out with the same method used in the optimization process.

2. Synthesis and Characterization

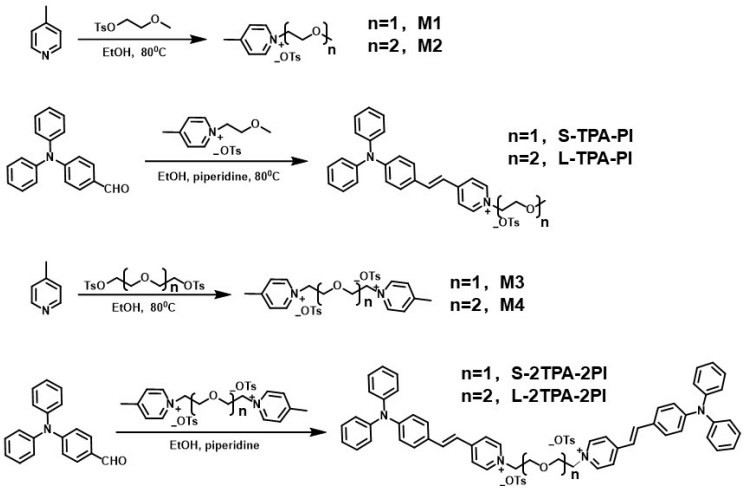

Scheme S1 Synthetic route to the four compounds

M1, **M2**, **M3**, **M4** were prepared according to the literatures [S1].

Synthesis of S-TPA-PI: To a refluxing solution of compound M1 (2.75 g, 8.51 mmol) in ethanol (15.0 mL), 4-(diphenylamino)benzaldehyde (2.32 g, 8.51 mmol) were added into the reaction system. After a further 12 h reflux, the orange red solid were precipitated and was recrystallized by ethanol (10.0 mL), affording S-TPA-PI (3.10 g, 63.2%) as orange red solid. ^{1}H NMR (400 MHz, DMSO-d_6), δ (ppm) (Supplementary Fig. 1): 8.774-8.756 (d, J = 7.20 Hz, 2H), 8.128-8.110 (d, J = 7.20 Hz, 2H), 7.933-7.892 (d, J = 16.40 Hz, 1H), 7.599-7.577 (d, J = 8.80 Hz, 2H), 7.457-7.437 (d, J = 8.00 Hz, 2H), 7.361-7.326 (t, J = 7.00 Hz, 4H), 7.292-7.252 (d, J = 16.24 Hz, 1H), 7.143-7.124 (t, J = 3.80 Hz, 2H), 7.106-7.050 (m, 6H), 6.913-6.891 (d, J = 8.76 Hz, 2H), 4.628-4.603 (t, J = 5.00 Hz, 2H), 3.765-3.741 (t, J = 4.80 Hz, 2H), 3.223 (s, 3H), 2.234 (s, 3H). ^{13}C NMR (100 MHz, DMSO-d_6), δ (ppm) (Supplementary Fig. 2): 153.98, 150.03, 146.70, 146.32, 144.85, 141.42, 138.08, 130.37, 130.28, 128.55, 126.01, 125.93, 125.04, 123.47, 121.19, 120.98, 70.72, 59.49, 58.70, 21.23. MS (ESI) (Supplementary Fig. 3): calcd for: $C_{27}H_{28}N_2O^+$ [M/z], 407.2118, found, 407.2152.

Synthesis of L-TPA-PI: To a refluxing solution of compound M2 (3.10 g, 8.44 mmol) in ethanol (15.0 mL), 4-(diphenylamino) benzaldehyde (2.31 g, 8.44 mmol) was added into the reaction system. After a further 24 h reflux, excess ethanol was removed under reduced pressure. The crude product was purified by silica gel column chromatography using CH_2Cl_2/CH_3OH=10:1 (v/v) as eluent, affording L-TPA-PI (4.60 g, 63.0%) as salmon pink solid. ^{1}H NMR (400 MHz, DMSO-d_6), δ

(ppm) (Supplementary Fig. 4): 8.770-8.753 (d, *J* = 6.80 Hz, 2H), 8.132-8.115 (d, *J* = 6.84 Hz, 2H), 7.942-7.901 (d, *J* = 16.20 Hz, 1H), 7.596-7.574 (d, *J* = 8.72 Hz, 2H), 7.461-7.441 (d, *J* = 8.08 Hz, 2H), 7.358-7.319 (t, *J* = 7.88 Hz, 4H), 7.296-7.252 (d, *J* = 16.20 Hz, 1H), 7.140-7.103 (t, *J* = 7.44 Hz, 2H), 7.087-7.055 (t, *J* = 6.38 Hz, 6H), 6.911-6.889 (d, *J* = 8.68 Hz, 2H), 4.620-4.597 (t, *J* = 4.70 Hz, 2H), 3.854-3.830 (t, *J* = 4.74 Hz, 2H), 3.518-3.495 (t, *J* = 4.60 Hz, 2H), 3.343-3.300 (d, *J* = 8.74 Hz, 2H), 3.132 (s, 3H), 2.240 (s, 3H). ^{13}C NMR (100 MHz, DMSO-d_6), δ (ppm) (Supplementary Fig. 5): 143.18, 140.04, 137.37, 137.11, 135.93, 133.12, 130.45, 124.31, 124.22, 120.82, 120.76, 120.04, 118.71, 116.96, 116.79, 77.28, 76.00, 75.40, 67.66, 66.89, 37.04. MS (ESI) (Supplementary Fig. 6): calcd for: $C_{30}H_{31}N_2O_2^+$ [M/z], 451.2380, found, 451.2423.

Synthesis of S-2TPA-2PI: To a refluxing solution of compound M3 (4.80 g, 8.00 mmol) in ethanol (20.0 mL), 4-(diphenylamino) benzaldehyde (2.18 g, 8.00 mmol) was added into the reaction system. After another 48 hours of reflux, the reaction solution was concentrated at reduced pressure. The crude products were purified by silica gel column chromatography using CH_2Cl_2/CH_3OH=10:1 (v/v) as eluent, affording S-2TPA-2PI (4.50 g, 50.7%) as red solid. ^{1}H NMR (400 MHz, DMSO-d_6), δ (ppm) (Supplementary Fig. 7): 8.649-8.635 (d, *J* = 6.96 Hz, 4H), 8.029-8.012 (d, *J* = 7.00 Hz, 4H), 7.873-7.833 (d, *J* = 16.20 Hz, 2H), 7.465-7.429 (m, 8H), 7.311-7.271 (t, *J* = 7.92 Hz, 8H), 7.189-7.148 (d, *J* = 16.24 Hz, 2H), 7.121-7.084 (t, *J* = 7.40 Hz, 4H), 7.068-7.047 (d, *J* = 8.28 Hz, 4H), 6.982-6.963 (d, *J* = 7.44 Hz, 8H), 6.828-6.806 (d, *J* = 8.76 Hz, 4H),4.581-4.558 (t, *J* = 4.62 Hz, 4H), 3.830-3.808 (t, *J* = 4.50 Hz, 4H), 2.230 (s, 6H). ^{13}C NMR (100 MHz, DMSO-d_6), δ (ppm) (Supplementary Fig. 8): 153.76, 149.89, 146.52, 146.33, 144.72, 141.40, 138.07, 130.30, 128.55, 128.32, 126.01, 125.80, 125.02, 123.24, 121.11, 120.77, 68.65, 59.61, 21.33. MS (ESI) (Supplementary Fig. 9): calcd for: $C_{54}H_{48}N_4O^{2+}$ [M/z], 384.1909, found, 384.1948.

Synthesis of L-2TPA-2PI: To a refluxing solution of compound M4 (2.80 g, 4.34 mmol) in ethanol (20.0 mL), 4-(diphenylamino) benzaldehyde (2.38 g, 8.69 mmol) was added into the reaction system. After a further 24 h reflux, excess ethanol was removed under reduced pressure. The crude product was purified by silica gel column chromatography using CH_2Cl_2/CH_3OH=10:1 (v/v) as eluent, affording L-2TPA-2PI (3.50 g, 69.9%) as red solid. ^{1}H NMR (400 MHz, DMSO-d_6), δ (ppm) (Supplementary Fig. 10): 8.716-8.699 (d, *J* = 6.92 Hz, 4H), 8.080-8.063 (d, *J* = 6.92 Hz, 4H), 7.866-7.825 (d, *J* = 16.16 Hz, 2H), 7.539-7.517 (d, *J* = 8.76 Hz, 4H), 7.459-7.439 (d, *J* = 8.12 Hz, 4H), 7.341-

7.302 (t, *J* = 7.90 Hz, 8H), 7.227-7.186 (d, *J* = 16.20 Hz, 2H), 7.134-7.097 (t, *J* = 7.40 Hz, 4H), 7.068-7.033 (t, *J* = 7.04 Hz, 14H), 6.873-6.851 (d, *J* = 8.72 Hz, 4H), 4.590-4.597 (t, *J* = 4.62 Hz, 4H), 3.813-3.790 (t, *J* = 4.66 Hz, 4H), 3.480 (s, 4H), 2.233 (s, 6H). ^{13}C NMR (100 MHz, DMSO-d_6), δ (ppm) (Supplementary Fig. 11): 153.88, 150.02, 146.65, 146.18, 144.82, 141.39, 138.17, 130.36, 130.27, 128.36, 126.02, 125.93, 125.06, 123.35, 121.09, 120.85, 69.98, 69.26, 59.46, 21.23. MS (ESI) (Supplementary Fig. 12): calcd for: $C_{56}H_{52}N_4O_2^{2+}$ [M/2], 406.2040, found, 406.2041.

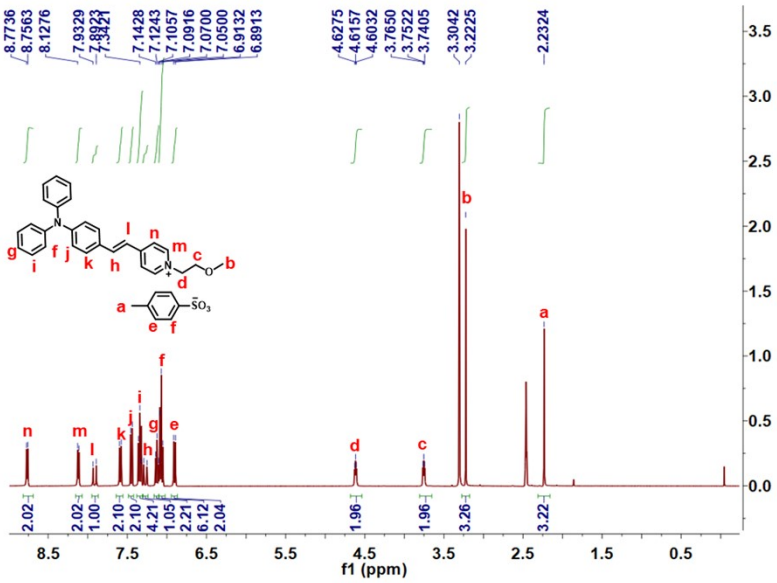

Fig. S1 ^{1}H-NMR spectrum of S-TPA-PI.

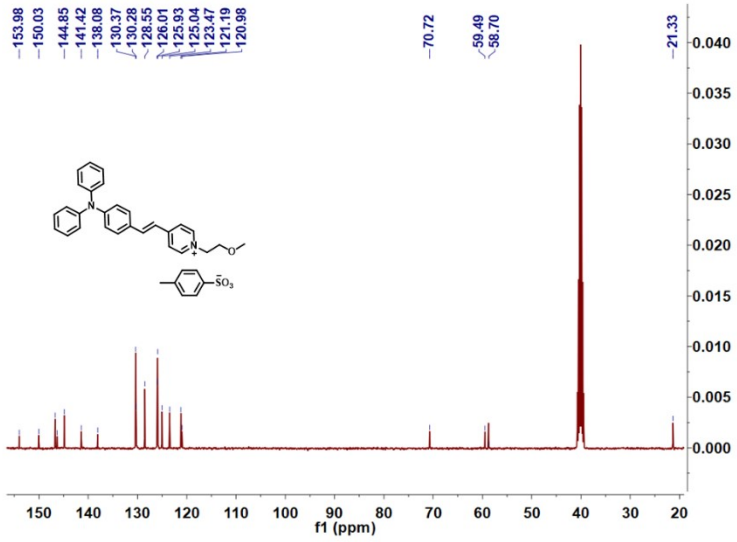

Fig. S2 ^{13}C-NMR spectrum of S-TPA-PI.

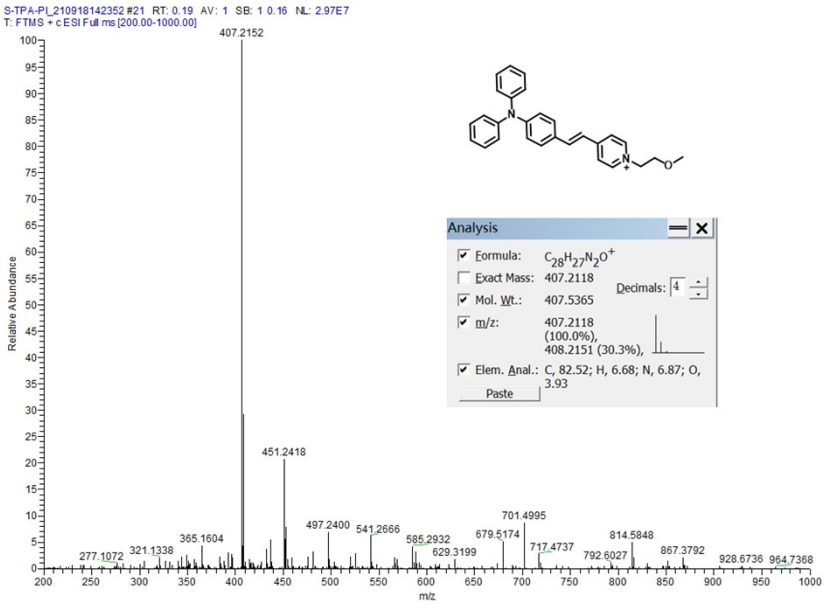

Fig. S3 ESI-Mass spectrum of S-TPA-PI.

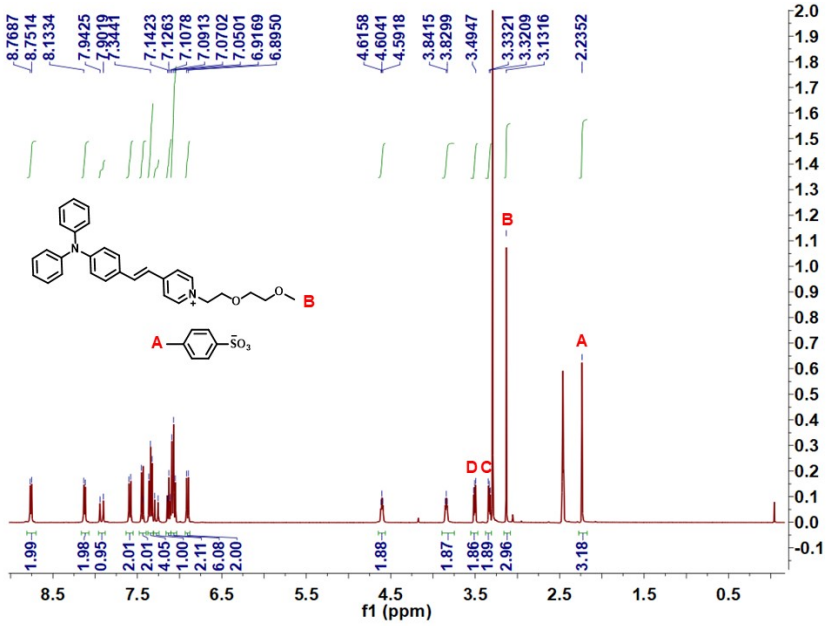

Fig. S4 ^{1}H-NMR spectrum of L-TPA-PI.

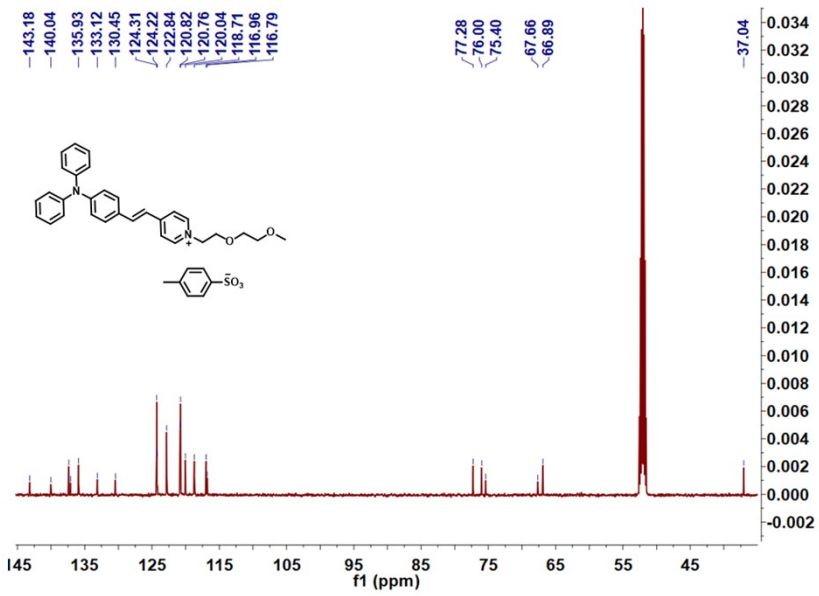

Fig. S5 ^{13}C-NMR spectrum of L-TPA-PI.

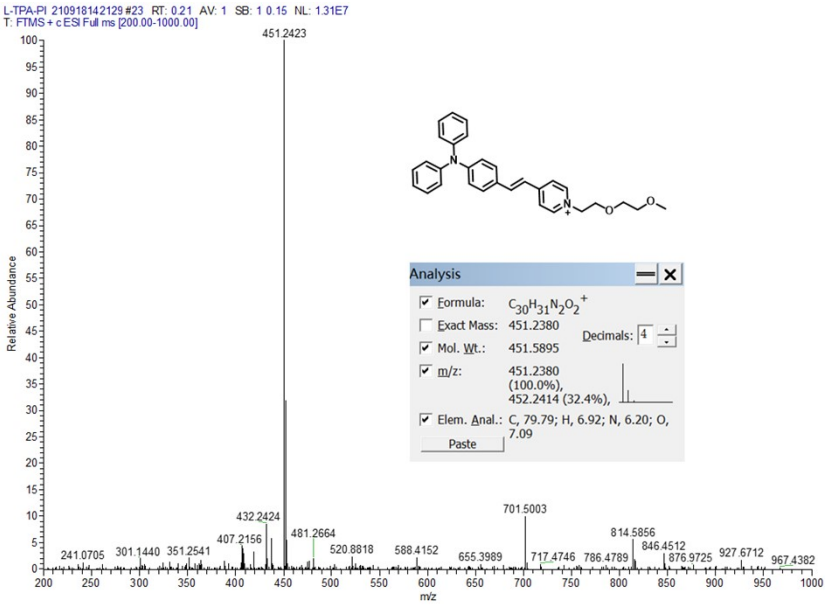

Fig. S6 ESI-Mass spectrum of L-TPA-PI.

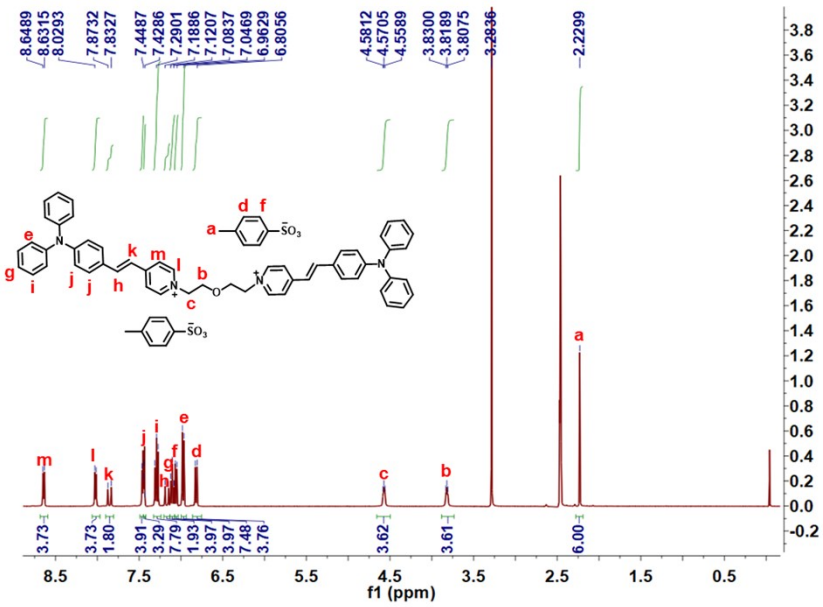

Fig. S7 ^{1}H-NMR spectrum of S-2TPA-2PI**.**

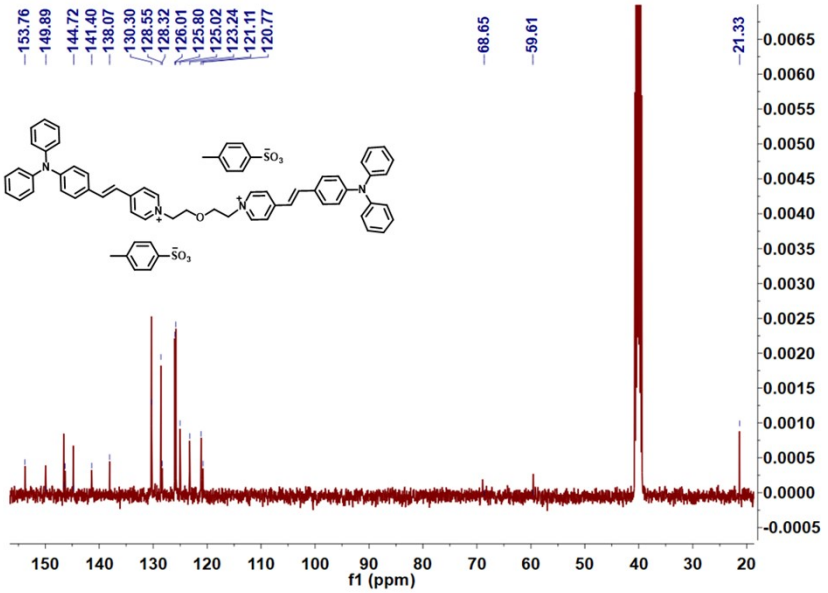

Fig. S8 ^{13}C-NMR spectrum of S-2TPA-2PI.

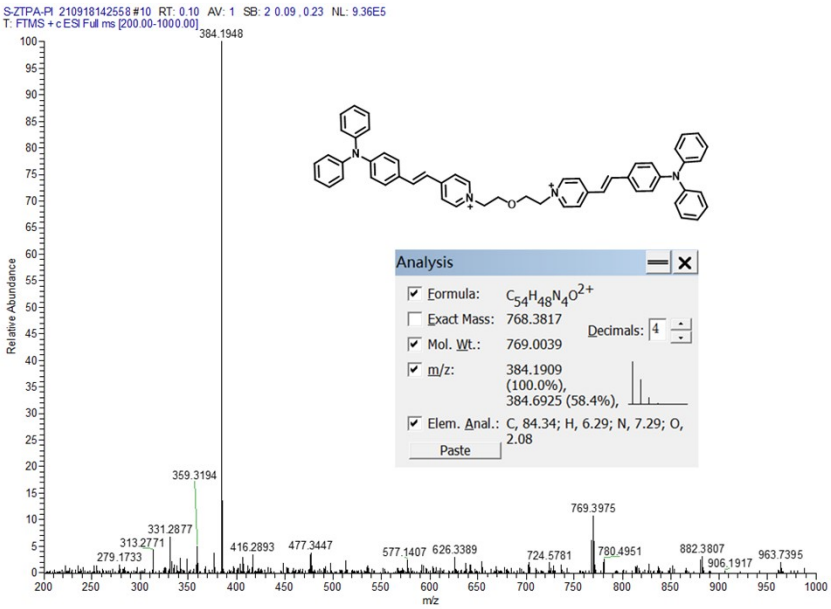

Fig. S9 ESI-Mass spectrum of S-2TPA-2PI.

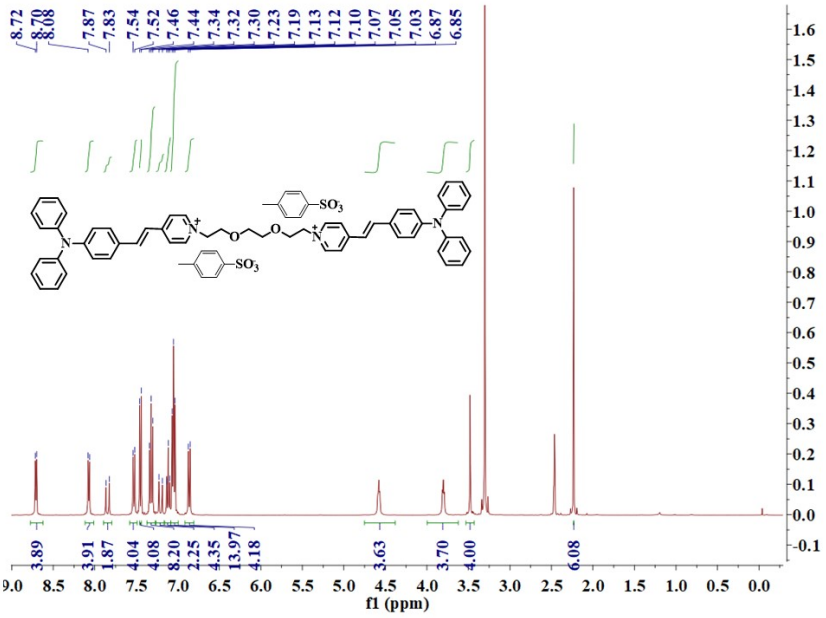

Fig. S10 ^{1}H-NMR spectrum of L-2TPA-2PI**.**

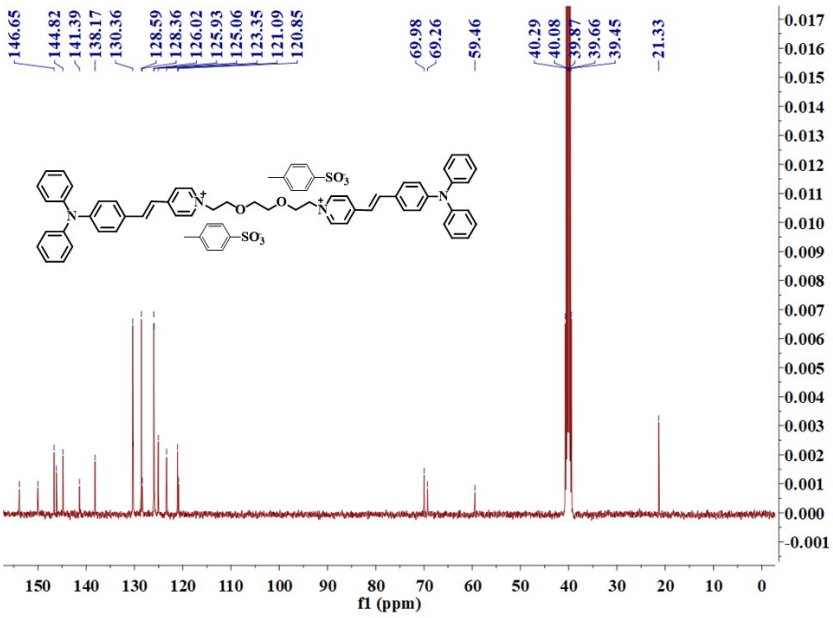

Fig. S11 ^{13}C-NMR spectrum of L-2TPA-2PI.

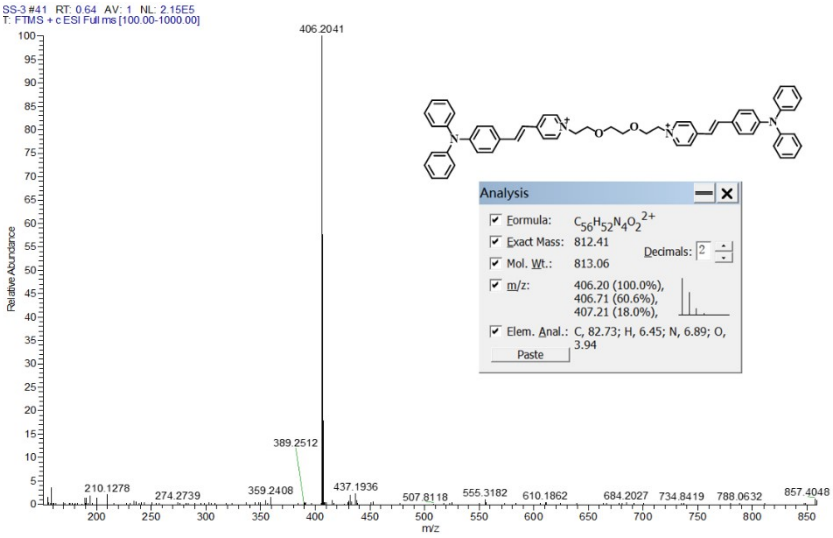

Fig. S12 ESI-Mass spectrum of L-2TPA-2PI.

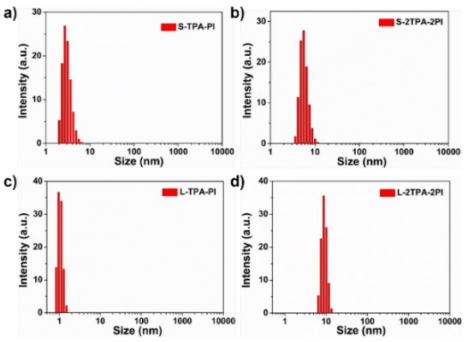

Fig. S13 Size distribution of S-TPA-PI, S-2TPA-2PI, L-TPA-PI, and L-2TPA-2PI in DMSO.

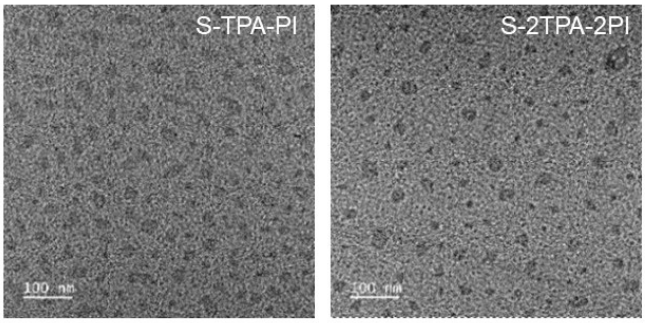

Fig. S14 The TEM of S-TPA-PI-aggregate and S-2TPA-2PI-aggregate. Scale bar: 100 nm.

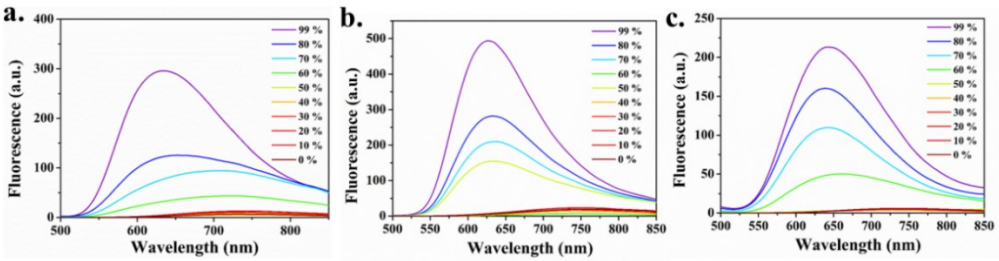

Fig. S15 Fluorescence spectra of a). S-TPA-PI, b). L-TPA-PI and c). L-2TPA-2PI in DMSO/water mixtures (0%, 10%, 20%, 30%, 40%, 50%, 60%, 70%, 80%, 90%, 100%) with different water (f_w), respectively.

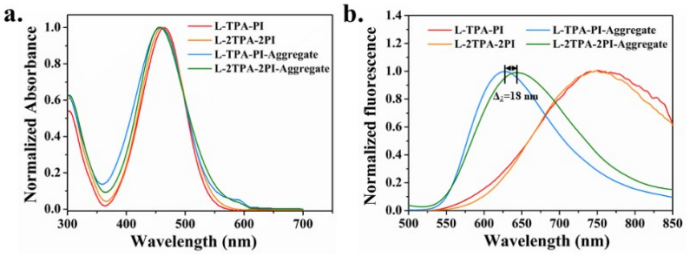

Fig. S16 a) The normalized absorbance and b) fluorescence spectra of L-TPA-PI and L-2TPA-2PI in DMSO or aqueous solution.

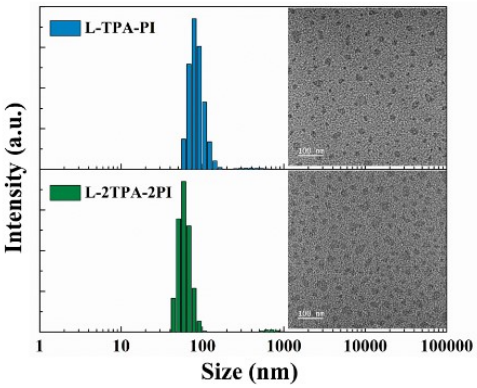

Fig. S17 Size distribution and morphology of L-TPA-PI-aggregate and L-2TPA-2PI-aggregate confirmed by DLS and TEM. Scale bar: 100 nm.

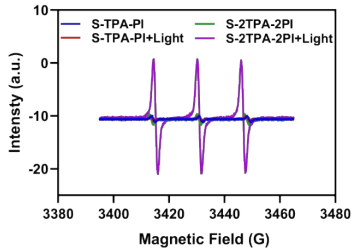

Fig. S18 The electron spin resonance spectra of TEMPO/S-TPA-PI and TEMPO/S-2TPA-2PI in aggregation under LED lamp irradiation (50 mW/cm^2) for 0 or 2 min.

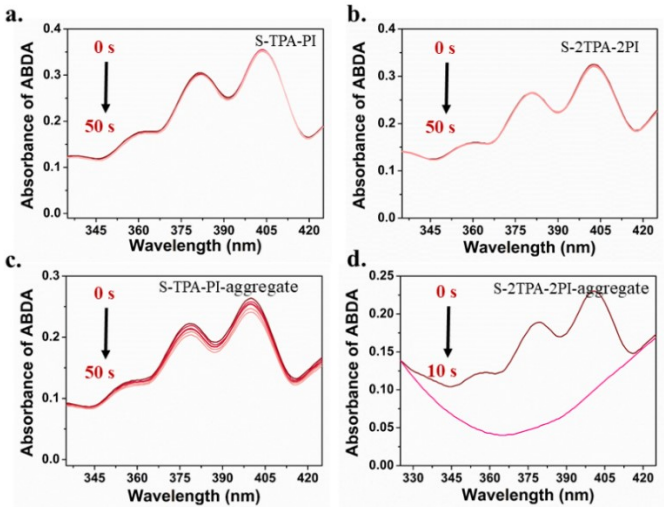

Fig. S19 a) ~d) The decomposition curves of ABDA in the presence of S-TPA-PI, S-2TPA-2PI in DMSO or H_2O under different irradiation time (LED light; 50 mW/cm^2).

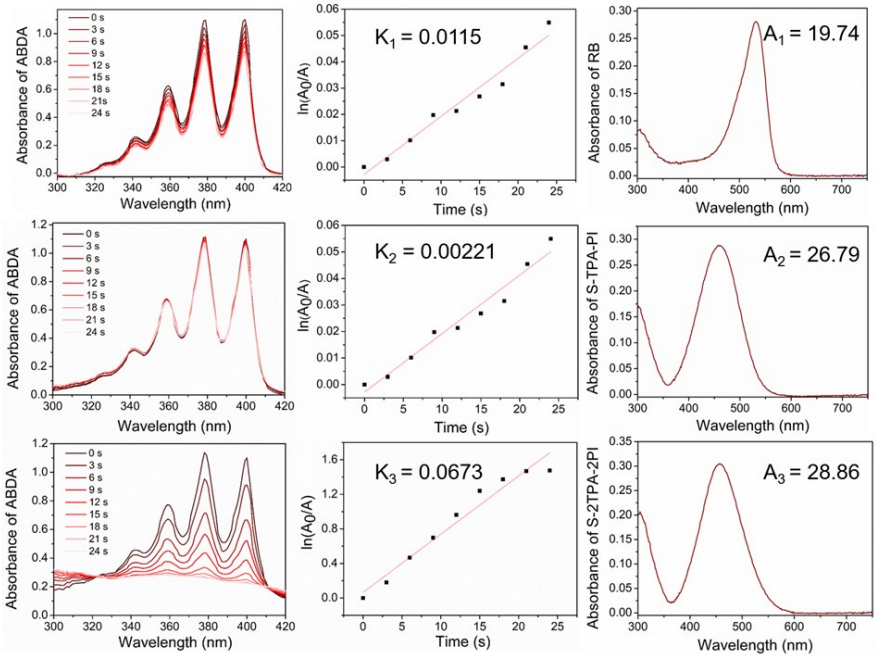

Fig. S20 The yield of $^1O_2$ for S-TPA-PI, S-2TPA-2PI in H_2O (RB as a reference).

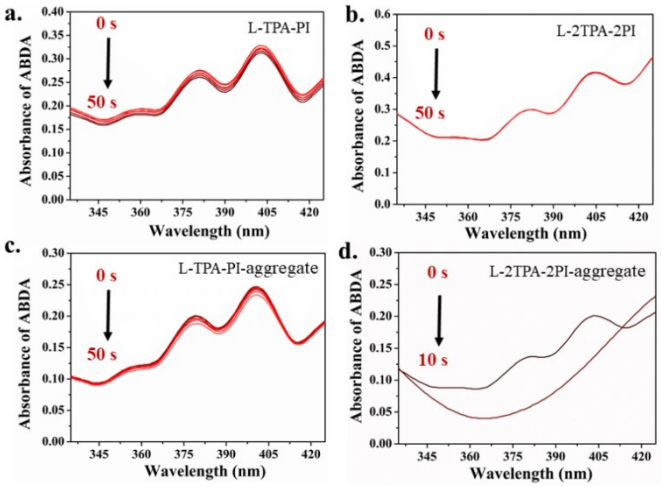

Fig. S21 a) ~d) The decomposition curves of ABDA in the presence of L-TPA-PI, L-2TPA-2PI in DMSO or H_2O under different irradiation time (LED light; 50 mW/cm^2).

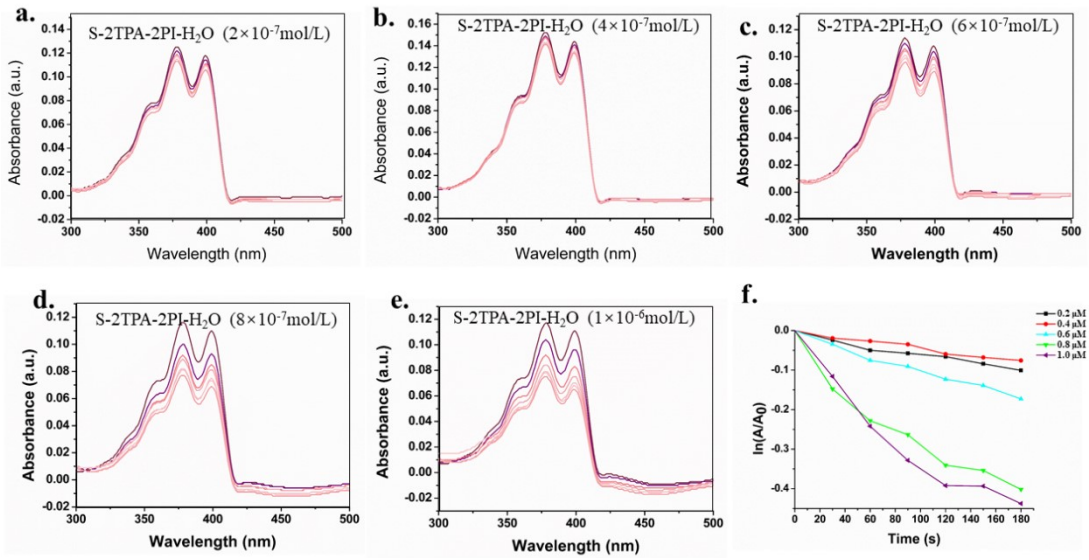

Fig. S22 The ability of $^1O_2$ generation in the presence of S-2TPA-2PI-aggregate with different concentration under different irradiation time (LED light; 50 mW/cm^2).

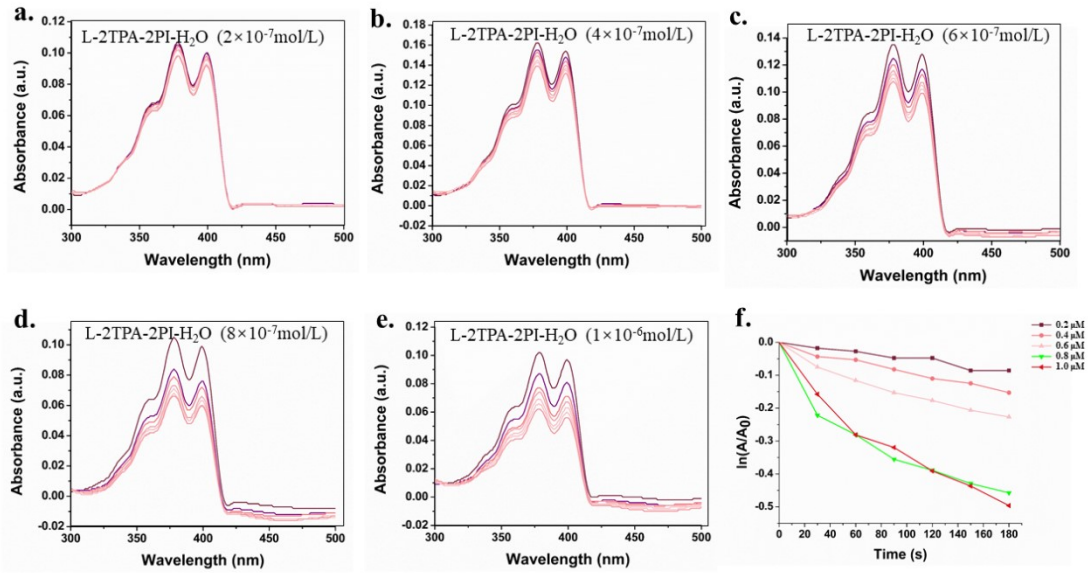

Fig. S23 The ability of $^1O_2$ generation in the presence of L-2TPA-2PI-aggregate with different concentration under different irradiation time (LED light; 50 mW/cm^2).

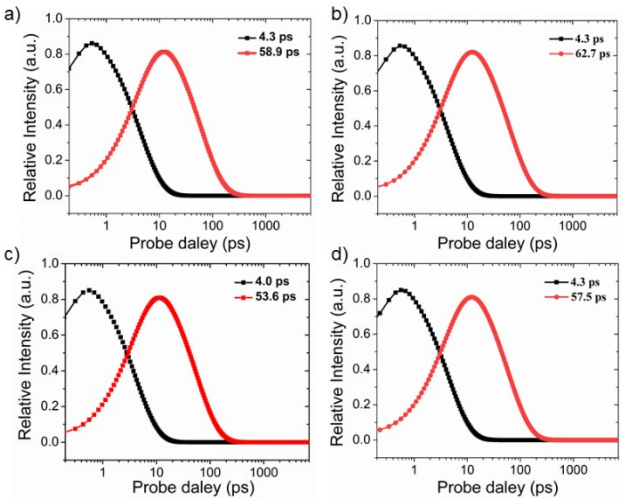

Fig. S24 The corresponding dynamics for excited state absorption of a) S-TPA-PI, b) L-TPA-PI, c) S-2TPA-2PI and d) L-2TPA-2PI in DMSO and argon atmosphere.

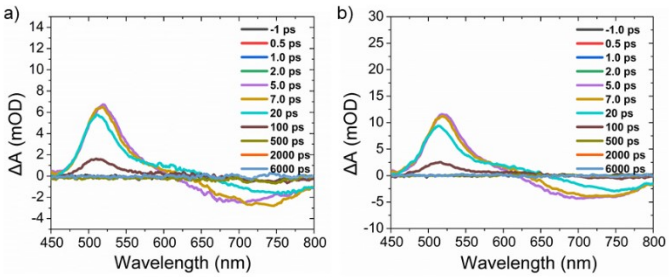

Fig. S25 The transient absorption spectra in DMSO and argon atmosphere of a) L-TPA-PI, b) L-2TPA-2PI.

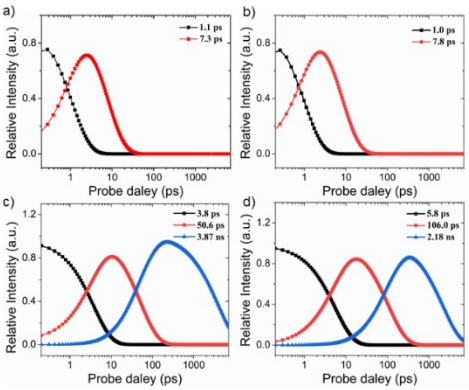

Fig. S26 The corresponding dynamics for excited state absorption of a) S-TPA-PI, b) L-TPA-PI, c) S-2TPA-2PI and d) L-2TPA-2PI in H_2O and argon atmosphere.

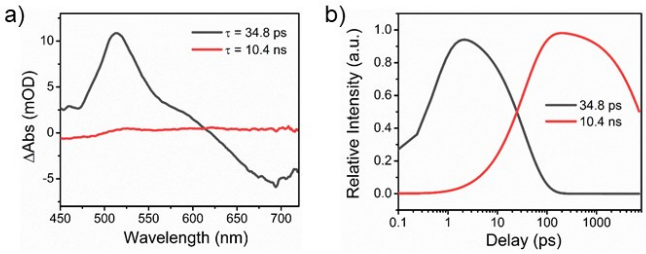

Fig. S27 The transient absorption spectra and corresponding dynamics for excited state absorption of S-TPA-PI@CB[8].

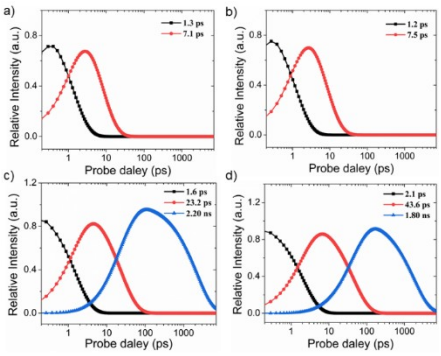

Fig. S28 The corresponding dynamics for excited state absorption of a) S-TPA-PI, b) L-TPA-PI, c) S-2TPA-2PI and d) L-2TPA-2PI in H_2O and air atmosphere.

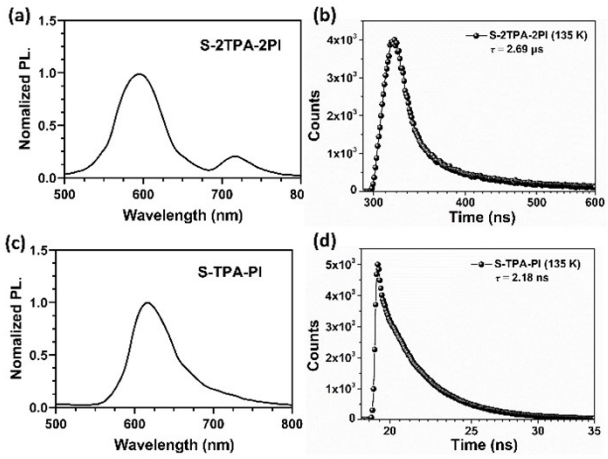

Fig. S29 (a) PL spectra of S-2TPA-2PI; (b) Temperature-dependent phosphorescent spectrum of S-2TPA-2PI; (c) PL spectra of S-TPA-PI; (d) Temperature-dependent phosphorescent spectrum of S-TPA-PI.

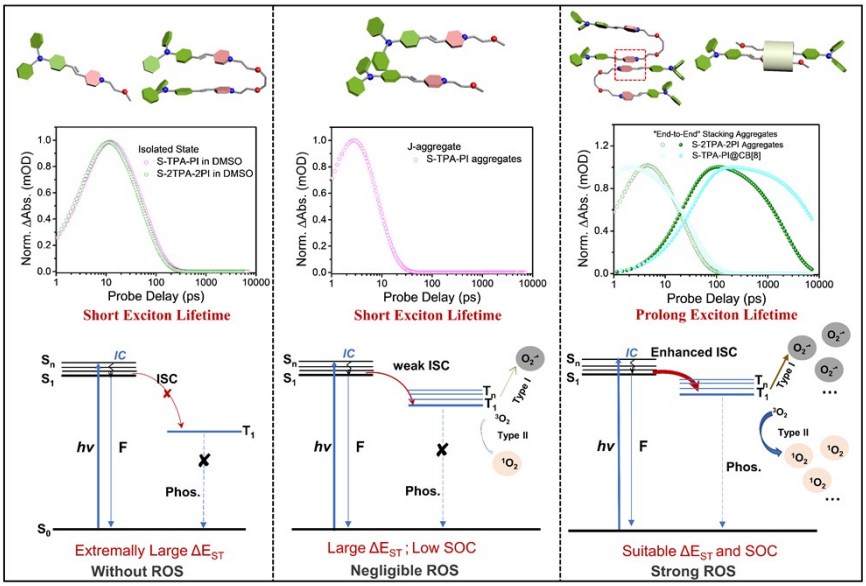

Fig. S30 The schematic diagram to describe the excited state processes to result in ROS initiated via isolated states (monomer or dimer), J-aggregate, "End to End" stacking (dimer or monomer+CB[8]).

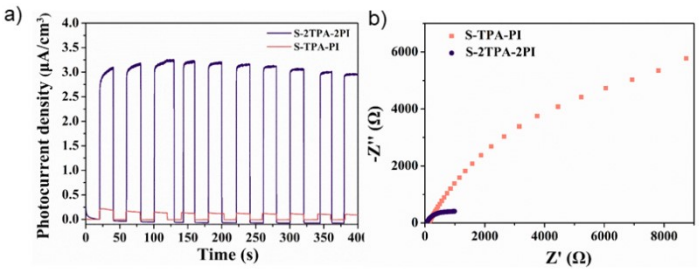

Fig. S31 The charge transfer resistance of S-TPA-PI-aggregate and S-2TPA-2PI-aggregate.

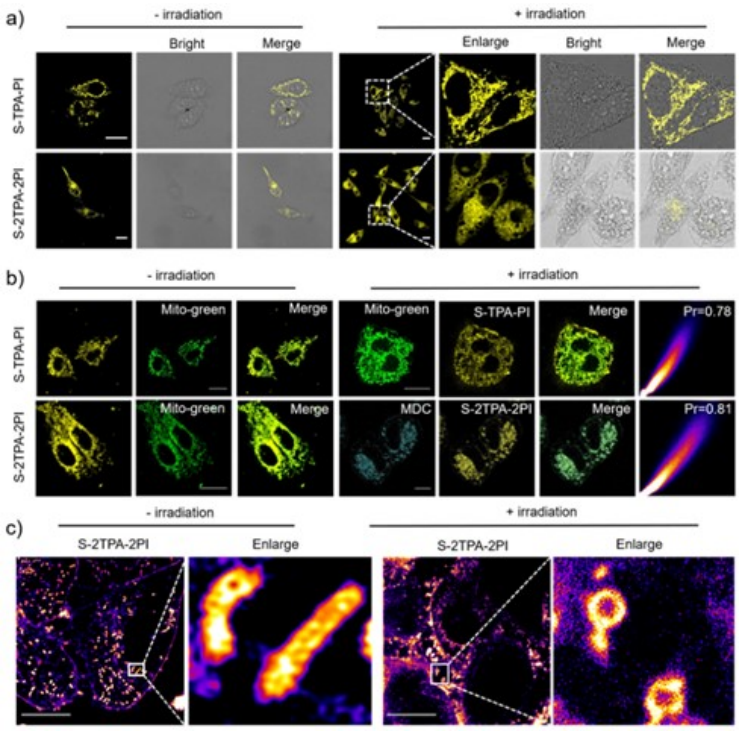

Fig. S32 (a). Confocal images of HepG2 cells treated with S-2TPA-2PI or S-TPA-PI, respectively. (b). Co-localization images of live HepG2 cells with S-2TPA-2PI or S-TPA-PI (10 μM) and Mito-Tracker Green or MDC (10 μM). (c). Airyscan images of HepG2 cells treated with S-2TPA-2PI. Yellow channel: λ_{ex} = 488 nm and λ_{em} = 560-640 nm and green channel: λ_{ex} = 488 nm and λ_{em} = 500-540 nm. Scale bar: 20 μm.

3. Supplementary Table

Table S1. Crystal data and structure refinement for the S-2TPA-2PI.

Crystal system	triclinic
Space group	P-1
a/Å	9.0104(4)
b/Å	13.7067(5)
c/Å	24.3591(9)
α/°	84.789(3)
β/°	81.573(3)
γ/°	89.490(3)
Volume/Å^3	2963.6(2)
Z	2
ρ_{calc}g/cm^3	1.301
μ/mm^{-1}	1.324
F(000)	1228.0

Radiation	Cu Kα (λ = 1.54186)
Index ranges	-10 ≤ h ≤ 7, -13 ≤ k ≤ 16, -27 ≤ l ≤ 28
Final R indexes [I>=2σ (I)]	R1 = 0.0475, wR2 = 0.1108
Final R indexes [all data]	R1 = 0.0765, wR2 = 0.1223

Table S2. Crystal data and structure refinement for the S-TPA-PI.

Crystal system	triclinic
Space group	P-1
a/Å	9.561(6)
b/Å	10.771(10)
c/Å	32.42(2)
α/°	89.714(12)
β/°	83.055(8)
γ/°	76.393(7)
Volume/Å^3	3220(4)
Z	4
ρ_{calc}g/cm^3	1.211
μ/mm^{-1}	0.142
F(000)	1242.0
Radiation	MoKα (λ = 0.71073)
Index ranges	-12 ≤ h ≤ 12, -13 ≤ k ≤ 13, -41 ≤ l ≤ 41
Final R indexes [I>=2σ (I)]	R1 = 0.1398, wR2 = 0.3571
Final R indexes [all data]	R1 = 0.2812, wR2 = 0.4413

4. References

[S1] F. Neese, *WIREs Comput. Mol. Sci.,* **2012**, 2, 73-78.

[S2] J. P. Perdew, *Phys. Rev. B*, **1986**, 33, 8822-8824.

[S3] A. D. Becke, Phys. Rev. A, **1988**, 38, 3098-3100.

[S4] F. Neese, *J. Comput. Chem.,* **2003**, 24, 1740-1747.

[S5] Q. Wu, Y. Li, Y. Li, D. Wang and B. Z. Tang, *Mater. Chem. Front.,* **2021**, 5, 3489-3496.